arXiv:1211.6935v1 [cond-mat.soft] 29 Nov 2012

Spontaneous autophoretic motion of isotropic particles

Sébastien Michelin,[1, *] Eric Lauga,[2, †] and Denis Bartolo[3, 4, ‡]
[1] *LadHyX – Département de Mécanique, Ecole polytechnique, 91128 Palaiseau Cedex, France*
[2] *Department of Mechanical and Aerospace Engineering,*
University of California San Diego, 9500 Gilman Drive, La Jolla CA 92093-0411, USA.
[3] *Laboratoire de Physique de l'Ecole Normale Supérieure de Lyon,*
Université de Lyon and CNRS, 46, allée dItalie, F-69007 Lyon, France
[4] *PMMH, CNRS UMR7636, ESPCI ParisTech, Université Pierre et Marie Curie,*
Université Paris Diderot, 10, rue Vauquelin, 75231 Paris Cedex 05, France
(Dated: November 30, 2012)

Suspended colloidal particles interacting chemically with a solute are able to self-propel by autophoretic motion when they are asymmetrically patterned (Janus colloids). Here we demonstrate that the chemical anisotropy is not a necessary condition to achieve locomotion. The non linear interplay between surface osmotic flows and solute advection can produce spontaneous, and self-sustained motion of isotropic particles. We solve, for a spherical particle, the classical nonlinear autophoretic theoretical framework at arbitrary Péclet number. For a given set of material parameters, there exists a critical particle size, or equivalently a critical Péclet number, above which spontaneous autophoretic motion occurs. The flow induced by the particle further displays a hierarchy of instabilities associated with quantized critical Péclet numbers. Using numerical solutions of the full (unsteady) diffusiophoretic problem we confirm our analytical predictions and show that, above the instability threshold, the isotropic particles reach a steady swimming state with broken front-back symmetry in the concentration field and the hydrodynamic signature of a "pusher" swimmer. This instability to propulsion could be relevant to the high-throughput production of self-propelled particles.

PACS numbers: 82.70.Dd, 47.70.Fw, 47.20.-k, 87.85.gj

The locomotion of microorganisms has long been used as a motivation and a practical inspiration for the design of synthetic self-propelled particles. Typically, biological cells generate propulsion by deforming their slender appendages, termed flagella or cilia, in a non-time-reversible fashion [1]. However, and perhaps not surprisingly given the numerous microfabrication challenges, no genuinely self-propelled micro-swimmer has been manufactured in the lab so far. Instead, man-made biomimetic propellers are driven by external torques or forces. That actuation allows either to deform soft propellers whose deformed shape induce propulsion [2–4], to continuously generate propulsion in chiral shapes [5, 6], or to exploit interactions with surfaces [7–9].

An alternative route for the production of artificial small-scale swimmers has proven to be much more successful. It consists in making miniaturized chemically powered "engines" with no moving parts, typically made of reactive Janus beads or rods [10–12]. The reaction products released by these chemically-asymmetric particles create concentration gradients which induce a net phoretic fluid motion near their surface leading to locomotion. Theoretically, the interest in these so-called autophoretic swimmers was triggered by a theoretical model which accounted for such a novel propulsion mechanism in a simple and generic fashion [13]. This model was then further elaborated to include the nonlinear interplay between the colloid motion and the advection of the reactants [14, 15], to deal with the rotational Brownian motion of the swimmers [16], and to detail the microscopic coupling between the concentration gradients and the fluid flows at small scales [17].

In order to self-propel, autophoretic swimmers are chemically patterned, and it is the asymmetries in the chemical reactions on the swimmer surface which are responsible for locomotion in the first place. This requirement would make it thus difficult to achieve high-throughput production. An ingenious solution to such an engineering issue was recently offered with the production of isotropic self-propelled Marangoni droplets [18]. In a mechanism akin to the one responsible for the spontaneous motion of reactive droplets surfing on fluid interfaces [19, 20], a net flow is induced around the droplets by interfacial stresses induced by self-generated gradients of reactive surfactants [18, 21]. Unlike autophoretic swimmers, which swim as a result of built-in asymmetries in their design, the concentration of surfactant molecules at the surface of reactive droplets is spontaneously broken, leading to propulsion.

In this letter we demonstrate that autophoresis can produce spontaneous motion of isotropic solid particles even in the absence of interfacial (Marangoni) stresses. We solve analytically the classical nonlinear autophoretic theoretical framework at arbitrary Péclet number for perturbation around the isotropic, purely diffusive, state. We show that, for a given set of material properties, there exists a critical particle size above which spontaneous autophoretic motion occurs. In addition, the flow induced by the reactive particles displays a hierarchy of instabilities associated with quantized critical Péclet numbers. Using numerical solutions of the full unsteady diffusiophoretic problem we confirm our analytical predictions and show that, above the instability threshold, isotropic particles reach, after a transient, a steady swimming state with broken front-back symmetry in the concentration field and the hydrodynamic signature of a "pusher" swimmer.

We consider a spherical particle of radius a located in a Newtonian fluid of shear viscosity η. We focus on the limit of steady Stokes flow so that the inertia of both the fluid and the particle is negligible. The sphere is chemically active and either emits or captures a single type of solute particles with an isotropic surface emission rate denoted $\mathcal{A}$ [13, 22]. Within the standard minimal framework, we ignore in what follows the specifics of the chemical reaction occurring at its surface, and all other reactants and reaction products, which are assumed to interact only weakly with the particle. The solute interacts with the spherical particle through a short-range potential. The competition between the interaction potential and molecular diffusion sets the thickness of the so-called diffuse layer, λ. As in classical approaches, we consider the thin-diffuse layer approximation, $\lambda \ll a$ [23].

Tangential gradients in solute concentration induce a net slip (phoretic) velocity outside the diffuse layer, together with a tangential (Marangoni) stress discontinuity at the particle surface [15, 23]. For a solid particle, Marangoni stresses vanish, and the phoretic slip velocity is set by the local chemical-potential gradient parallel to the surface [24]. For small variations of the concentration, $c(\mathbf{r}, t)$, its azimuthal component is given by

$$u_\theta(r = a) = \frac{\mathcal{M}}{a}\frac{\partial c}{\partial \theta}\cdot \tag{1}$$

The mobility, $\mathcal{M} \sim \pm k_B T \lambda^2/\eta$, can either be positive or negative depending of the form of the solute-surface interactions (k_B is the Boltzmann constant, and T the temperature) [23]. Assuming that the solute has a molecular diffusivity $\mathcal{D}$, the typical autophoretic velocity which sets the swimming speed of a Janus colloid is $\mathcal{V} = |\mathcal{A}\mathcal{M}|/\mathcal{D}$ [22]. Non-dimensionalizing velocities, lengths, and concentrations in the transport equations by $\mathcal{V}$, a, and $a|\mathcal{A}|/\mathcal{D}$ respectively, the coupled fluid flow-solute advection-diffusion problem takes the form

$$\nabla^2 \mathbf{u} = \nabla p, \qquad \nabla\cdot\mathbf{u} = 0, \tag{2}$$

$$|\mathrm{Pe}|\left(\frac{\partial c}{\partial t} + \mathbf{u}\cdot\nabla c\right) = \nabla^2 c, \tag{3}$$

where we have defined the (signed) Péclet number as $\mathrm{Pe} = \mathcal{A}\mathcal{M}a/\mathcal{D}^2$. We henceforth consider axisymmetric solutions only, so that in spherical polar coordinates the solute concentration is written as $c(r, \mu, t)$ with $\mu \equiv \cos\theta$, and only rectilinear motion along the axis of symmetry $\mathbf{e}_z$ is considered. In dimensionless units, the surface activity and the particle mobility become unitary numbers, $A = \mathcal{A}/|\mathcal{A}| = \pm 1$, $M = \mathcal{M}/|\mathcal{M}| = \pm 1$, and the boundary conditions on the particle surface become

$$\mathbf{u}(r\to\infty) = -U\mathbf{e}_z, \quad c(r\to\infty) = c_\infty, \tag{4}$$

$$\frac{\partial c}{\partial r}(r = 1) = -A, \tag{5}$$

$$u_r(r = 1) = 0, \tag{6}$$

$$u_\theta(r = 1) = -M\sqrt{1-\mu^2}\,\frac{\partial c}{\partial \mu}(r = 1). \tag{7}$$

In Eq. (4), $U(t)$ is the dimensionless swimming velocity, obtained by enforcing that the particle is force-free. Using the reciprocal theorem, $U(t)$ is found to be the surface average of the slip velocity [22, 25] and, using Eq. (1), is written in terms of the first moment of $c(1, \mu, t)$ only as

$$U(t) = -M\int_{-1}^{1} \mu\, c(1, \mu, t)\,\mathrm{d}\mu. \tag{8}$$

The dimensionless problem is then fully characterized by the signs of both A and M, the far-field concentration, c_∞, and the value of $|\mathrm{Pe}|$.

In the case of uniform surface activity (constant value of A), a trivial solution exists at all Pe numbers, namely the solute concentration is isotropic, $\bar{c} = A/r + c_\infty$, leading to no net flow ($\bar{\mathbf{u}} = 0$) and zero swimming velocity ($\bar{U} = 0$). However, both the solute transport equation, Eq. (3), and the boundary conditions on the particle, Eq. (7), couple the swimming problem with the solute dynamics. A small fluctuation of the particle velocity would result in a polar perturbation of the flow field. Due to the nonlinear convective coupling, $\mathbf{u}\cdot\nabla c$, this velocity fluctuation would lead to a polarization of the concentration field around the finite-size particle. In turn, the first moment of the surface concentration, $c(1, \mu, t)$, would become finite and, depending on its sign in relation to the initial perturbation, increase or decrease the particle velocity through Eq. (8). If the velocity decreased, the initial perturbation would be stabilized, and no net motion could occur as a result of an infinitesimal fluctuation. However, if the velocity increased, the broken symmetry in the solute concentration would be amplified, and spontaneous motion would occur.

To quantify the conditions for spontaneous motion, we analytically investigate the stability of the isotropic state. Defining $c = \bar{c} + c'$, $\mathbf{u} = \mathbf{u}'$, $U = U'$, and subsequently dropping the primes to denote perturbations, the Stokes flow problem around the sphere can be solved analytically using the decomposition of the slip velocity along the so-called squirming modes [26, 27]. We then project both the advection-diffusion equation and the definition of the slip velocity along these modes, and take the first moment of the resulting equation with respect to the angular dependence, μ. This leads to an inhomogeneous eigenvalue problem for the first moment of the concentration profile, $c_1(r,t) \equiv \frac{3}{2}\int_{-1}^{1} \mu\, c(r,\mu,t)\,\mathrm{d}\mu$, as

$$|\mathrm{Pe}|\frac{\partial c_1}{\partial t} - \frac{1}{r^2}\left[\frac{\partial}{\partial r}\left(r^2\frac{\partial c_1}{\partial r}\right) - 2c_1\right] = \frac{U\mathrm{Pe}}{r^2}\left(\frac{1}{r^3}-1\right), \tag{9}$$

$$U = -\frac{2}{3}Mc_1(1), \quad c_1'(1) = 0. \tag{10}$$

Note from Eq. (8) that the first moment, c_1, evaluated at $r=1$ is proportional to the instantaneous swimming speed of the particle, (Eq. 10). Looking for eigenmodes of the form $c_1(r,t) = \mathrm{e}^{\sigma t}c(r)$, it can be shown that all eigenvalues σ of Eqs. (9)–(10) are real, and that any $\sigma < 0$ is a solution. We focus here exclusively on potential unstable modes ($\sigma > 0$) and define $\beta \equiv \sqrt{\sigma|\mathrm{Pe}|} > 0$. Introducing the rescaled radial variable $x \equiv \beta r$, the function $C(x) \equiv c(r/\beta)$ satisfies

$$\frac{\mathrm{d}}{\mathrm{d}x}\left(x^2\frac{\mathrm{d}C}{\mathrm{d}x}\right) - \left(2+x^2\right)C = \frac{2\mathrm{Pe}}{3}\left(\frac{\beta^3}{x^3}-1\right). \tag{11}$$

The general solution of Eq. (11) satisfying the far-field condition $C(x\to\infty) = 0$ is

$$C(x) = \frac{2\mathrm{Pe}}{3}\left\{\frac{1}{x^2} + \beta^3\left[\frac{A(x)}{8x^2} + \frac{B(x)}{8x} + \frac{1}{4x^3}\right]\right\} + \frac{b\mathrm{e}^{-x}(1+x)}{x^2} \tag{12}$$

where b is an integration constant to be determined, and $A(x) = \sinh(x)\mathrm{Chi}(x) - \cosh(x)\mathrm{Shi}(x)$, and $B(x) = \sinh(x)\mathrm{Shi}(x) - \cosh(x)\mathrm{Chi}(x)$, with $\mathrm{Chi}(x)$ and $\mathrm{Shi}(x)$ being the hyperbolic cosine and sine integral functions respectively [28]. Applying the two boundary conditions on the sphere, $C'(\beta) = 0$, and $C(\beta) = 1$, and using the definitions of $A(x)$ and $B(x)$ yields a final implicit expression for the growth rate, $\sigma = \beta^2/|\mathrm{Pe}|$, as a function of the signed Péclet number

$$\mathrm{Pe} = \frac{12\beta^2 + 24\beta + 24}{\beta^4\displaystyle\int_\beta^\infty \frac{\mathrm{e}^{\beta - t}}{t}\mathrm{d}t + 6 + \beta^2 - \beta^3 - 2\beta}. \tag{13}$$

For positive values of β, the right-hand side of Eq. (13) is strictly greater than 4. For any value of Pe above this critical value, a single positive value of β exists such that Eq. (13) is satisfied. Consequently, the fluctuations of the first moment, c_1, and the particle swimming speed, U, are exponentially amplified if the condition $\mathrm{Pe} \geq \mathrm{Pe}_1 = 4$ is satisfied. Given that Pe is a signed quantity, the instability condition requires that $MA = 1$. Particles with positive (resp. negative) mobility $\mathcal{M}$ are unstable only if they have a positive (resp. negative) flux $\mathcal{A}$ corresponding to the case of emitting (resp. absorbing) the solute on the particle surface. The growth rate of the unstable swimming mode is shown as a function of Pe in Fig. 1 (solid line). From a practical point, the existence of critical Peclet number implies that there exists a critical particle radius, $a_1 = 4\mathcal{D}/\mathcal{V}$, above which an isotropic reactive particle at rest would undergo spontaneous motion. For instance, considering the prototypal example of a Pt-coated bead in a $\mathrm{H_2O/H_2O_2}$ solution, we have $\mathcal{V} \approx 20\,\mu\mathrm{m\,s^{-1}}$ [10, 22, 29] and taking $\mathcal{D} \approx 10^{-9}\,\mathrm{m^2/s}$ [30] we obtain a critical radius $a_1 \approx 100\,\mu\mathrm{m}$, which is experimentally accessible. This critical particle radius could be further reduced either by increasing the fluid viscosity, or by using reactants molecules with a larger molecular weight [11].

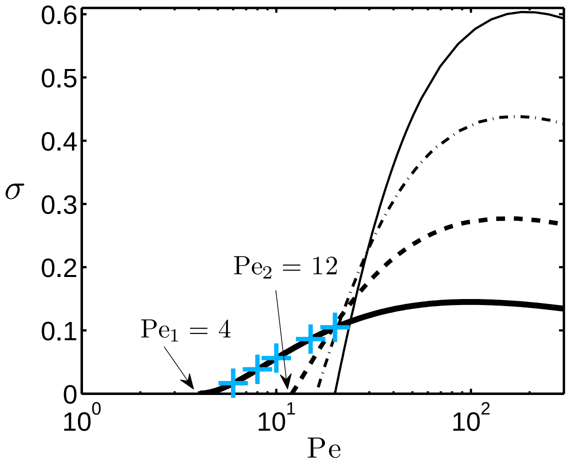

FIG. 1: (Color online) Growth rate of the unstable swimming mode (theoretical prediction, solid line) as a function of the Péclet number, Pe, for emitting particles ($A = 1$) and positive mobility ($M = 1$). Spontaneous symmetry-breaking of the concentration field and swimming occur at Pe = 4. The crosses represent the growth rate of the swimming mode $n = 1$ as obtained from numerical simulations of the full unsteady coupled problem. The growth rate of the unstable modes of azimuthal order $n = 2$, 3 and 4 are also shown (theoretical prediction, dashed, dash-dotted and thin-solid, respectively). Note that the hierarchy in the growth rates is reversed at high Pe.

In order to further investigate the possibility for long-time self-propulsion, we need to go beyond the above linear stability analysis and check whether the asymptotic state of the concentration field is compatible with swimming. In order to do so, numerical simulations of the full unsteady diffusiophoretic problem, Eqs. (2)–(7), are performed: the Stokes flow problem is solved explicitly using the squirming mode decomposition, and the advection-diffusion problem is marched in time using a semi-explicit scheme, finite differences in the radial directions, and the Legendre spectral decomposition for the azimuthal dependence [31]. A small velocity perturbation is imposed on the spherical particle initially at rest. Regardless of the amplitude of the initial perturbation, the system is stable and returns to its initial rest

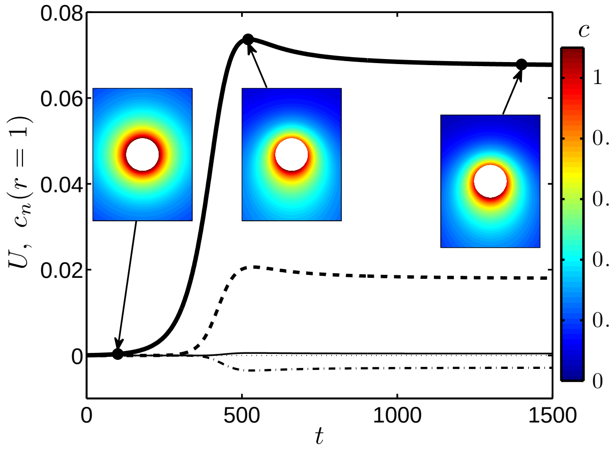

FIG. 2: (Color online) Time-evolution of the instantaneous swimming velocity $U(t)$ (thick solid line), and of three higher squirming modes, $c_n(r = 1, t)$: mode $n = 2$, which corresponds to the magnitude of the induced stresslet (dashed line), $n = 3$ (dash-dotted line) and $n = 4$ (thin solid line). Results are displayed for $\mathrm{Pe} = 6$ and $AM = 1$. The solute concentration is shown at three different times revealing the establishment of a front-back asymmetry for an upward swimming motion.

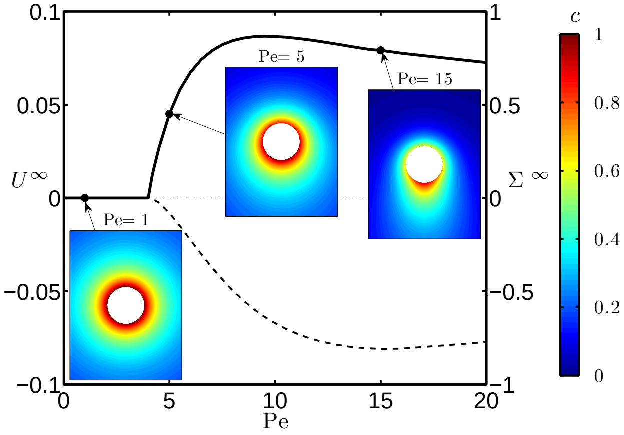

FIG. 3: (Color online) Long-time spontaneous swimming velocity, U^∞ (solid line), and magnitude of the long-time induced stresslet, $\Sigma^\infty \equiv -4\pi M c_2(r = 1, t = \infty)$ (dashed line), as a function of the Péclet number (with $AM = 1$). The steady state solute distribution around the particle is shown for $\mathrm{Pe} = 1$, $\mathrm{Pe} = 5$, and $\mathrm{Pe} = 15$ for an upward swimming motion. The swimmer is always a "pusher" in the far field.

state after perturbation for $\mathrm{Pe} < 4$. In contrast, when $\mathrm{Pe} > 4$, the swimming velocity of the particle grows exponentially, and the growth rates obtained numerically are in quantitative agreement with our analytic predictions, see Fig. 1.

Turning to the long-time behavior, our computations confirm that the asymptotic state of the concentration field is compatible with locomotion. This is illustrated in Fig. 2 for $\mathrm{Pe} = 6$, where we plot the time-evolution of the instantaneous particle swimming speed (thick solid line). A movie (supplementary information) and three typical snapshots in Fig. 2 illustrate the corresponding evolution of the solute concentration field. A steady state is reached and the swimming speed plateaus to a finite value in the long-time limit. Repeating the simulations for a range of Péclet numbers, we plot in Fig. 3 the nonlinear variation of the long-time swimming velocity, U^∞, as a function of Pe, demonstrating in particular the supercritical nature of the autophoretic instability. Note the non-monotonic variation with an optimal value of $\mathrm{Pe} \approx 9$ leading to the highest asymptotic swimming speed. For a given set of material parameters, and unlike autophoretic Janus particles [22], the swimming speed here explicitly depends on the particle radius $a \propto \mathrm{Pe}$. Physically, this difference arises because the concentration gradient around an isotropic particle is not merely set by the particle size but instead by a dynamical scale.

So far we focused exclusively on the impact of the concentration field on the particle swimming speed. In order to address their collective dynamics, one would need to gain insight on the associated flow field away from the particle. The higher-order squirming modes are defined as $c_n(r,t) = (n + 1/2)\int_{-1}^{1} c(r, \mu, t)L_n(\mu)\mathrm{d}\mu$, where $L_n(\mu)$ is the Legendre polynomial of order n. As discussed above, c_1 is the (only) swimming mode. The flow field associated with the mode c_2 is the one with the slowest spatial decay, that of a stresslet (i.e. of a force dipole) [32]. Higher values of n correspond to higher-order flow singularities in the far field. Repeating, for $n \geq 2$, the theoretical approach presented above for $n = 1$, we can obtain the unstable growth rates of each mode as a function of Pe. The results reveal a hierarchy of supercritical instabilities corresponding to an infinite set of quantized critical Péclet numbers, $\mathrm{Pe}_n = 4(n+1)$, for mode n. This hierarchy of instabilities is illustrated in Fig. 1 where we plot the dependence of the growth rates for modes 2, 3, and 4 on the Péclet number. Notably, the stresslet mode becomes unstable at $\mathrm{Pe}_2 = 12$.

Beyond linear analysis, the saturation of the swimming velocity results from the nonlinear evolution of concentration fluctuations having a $n = 1$ symmetry into higher-order n-modes, as shown in Fig. 2. Although the Péclet number is below the critical value for all modes but the first one to be unstable ($\mathrm{Pe} = 6$ in Fig. 2), the nonlinear dynamics leads non-zero values for the other modes (modes 2, 3, and 4 are shown in Fig. 2). In particular, the long-time value of the induced stresslet, Σ^∞, is shown in Fig. 3. Independently of the signs of both $\mathcal{A}$ and $\mathcal{M}$, the unstable particle induces in the far field a flow with the symmetry of a "pusher" swimmer, similarly to flagellated bacteria [1].

Similarly to Marangoni flows which have been observed for over 200 years to trigger the self-propulsion of camphor boats floating on water, in this letter we demonstrated that self-phoretic flows past isotropic particles show an instability to a spontaneous swimming state. The phenomenon discovered here could be exploited to design self-propelled "submarines" out of isotropic colloidal particles. The instability mechanism is expected to be applicable generically to particles of different shapes or interacting with many chemical species, and suggests a simple experimental model system to carry out physical studies of active systems.

We acknowledge valuable discussions with Olivier Dauchot and John Brady. This work was supported in part by the NSF through grant number CBET-0746285 (EL).

---

[*] Electronic address: sebastien.michelin@ladhyx.polytechnique.fr
[†] Electronic address: elauga@ucsd.edu
[‡] Electronic address: denis.bartolo@ens-lyon.fr

[1] E. Lauga and T. Powers, Rep. Prog. Phys. **72**, 096601 (2009).

[2] R. Dreyfus, J. Baudry, M. L. Roper, M. Fermigier, H. A. Stone, and J. Bibette, Nature **437**, 862 (2005).

[3] W. Gao, S. Sattayasamitsathit, K. M. Manesh, D. Weihs, and J. Wang, J. Am. Chem. Soc. **132**, 14403 (2010).

[4] O. S. Pak, W. Gao, J. Wang, and E. Lauga, Soft Matter **7**, 8169 (2011).

[5] A. Ghosh and P. Fischer, Nano Lett. **9**, 2243 (2009).

[6] S. Tottori, L. Zhang, F. Qiu, K. K. Krawczyk, A. Franco-Obregon, and B. J. Nelson, Adv. Mat. **24**, 811816 (2012).

[7] P. Tierno, O. Güell, F. Sagués, R. Golestanian, and I. Pagonabarraga, Phys. Rev. E **81**, 011402 (2010).

[8] C. E. Sing, L. Schmid, M. F. Schneider, T. Franke, and A. Alexander-Katz, Proc. Natl. Acad. Sci. USA **107**, 535 (2010).

[9] L. Zhang, T. Petit, Y. Lu, B. E. Kratochvil, K. E. Peyer, J. L. Ryan Pei, and B. J. Nelson, ACS Nano **4**, 6228 (2010).

[10] J. R. Howse, R. A. L. Jones, A. J. Ryan, T. Gough, R. Vafabakhsh, and R. Golestanian, Phys. Rev. Lett. **99**, 048102 (2007).

[11] S. J. Ebbens and J. R. Howse, Soft Matter **6**, 726 (2010).

[12] G. Zhao and M. Pumera, Chem. Asian J. **7**, 1994 (2012).

[13] R. Golestanian, T. B. Liverpool, and A. Ajdari, Phys. Rev. Lett. **94**, 220801 (2005).

[14] J. F. Brady, J. Fluid Mech. **667**, 216 (2010).

[15] F. Jülicher and J. Prost, Eur. Phys. J. E **29**, 27 (2009).

[16] R. Golestanian, Phys. Rev. Lett. **102**, 188305 (2009).

[17] B. Sabass and U. Seifert, J. Chem. Phys. **136**, 214507 (2012).

[18] S. Thutupalli, R. Seemann, and S. Herminghaus, New J. Phys. **13**, 073021 (2011).

[19] Y. Sumino, N. Magome, T. Hamada, and K. Yoshikawa, Phys. Rev. Lett. **94**, 068301 (2005).

[20] T. Toyota, N. Maru, M. M. Hanczyc, T. Ikegami, and T. Sugawara, J. Am. Chem. Soc. **131**, 5012 (2009).

[21] A. K. Schmid, N. C. Bartelt, and R. Q. Hwang, Science **290**, 1561 (2000).

[22] R. Golestanian, T. B. Liverpool, and A. Ajdari, New J. Phys. **9**, 126 (2007).

[23] J. L. Anderson, Ann. Rev. Fluid Mech. **21**, 61 (1989).

[24] D. C. Prieve and R. Roman, J. Chem. Soc. Far. Trans. **83**, 1287 (1987).

[25] H. A. Stone and A. D. T. Samuel, Phys. Rev. Lett. **77**, 4102 (1996).

[26] J. R. Blake, J. Fluid Mech. **46**, 199 (1971).

[27] S. Michelin and E. Lauga, Phys. Fluids **23**, 101901 (2011).

[28] M. Abramowitz and I. A. Stegun, *Handbook of Mathematical Functions with Formulas, Graphs, and Mathematical Tables* (Dover, New York, 1964).

[29] J. Palacci, C. Cottin-Bizonne, C. Ybert, and L. Bocquet, Phys. Rev. Lett. **105**, 088304 (2010).

[30] D. M. H. Kern, Journal of the American Chemical Society **76**, 4208 (1954).

[31] S. Michelin and E. Lauga, J. Fluid Mech. (2012), (in press).

[32] G. K. Batchelor, J. Fluid Mech. **41**, 545 (1970).